

Analysis of grain boundary sinks and interstitial diffusion in neutron-irradiated SiC

Sosuke Kondo,* Yutai Katoh, and Lance L. Snead

Materials Science and Technology Division, Oak Ridge National Laboratory, P.O. Box 2008, Oak Ridge, Tennessee 37831, USA

(Received 6 August 2010; revised manuscript received 18 October 2010; published 22 February 2011)

The widths of the interstitial loop denuded zone (DZ) along grain boundaries were examined for 3C-SiC irradiated at 1010–1380 °C by transmission electron microscopy (TEM) in an effort to obtain the activation energy of interstitial migration. Denuded-zone widths as small as 17 nm were observed below 1130 °C, indicating that a substantial population of “TEM invisible” voids of diameter <0.7 significantly contribute to interstitial annihilation. By using the obtained loop DZ width and the matrix sink strength (including the invisible voids), the activation energy of interstitial diffusion was determined to be 1.5 eV for the slower moving Si interstitial of SiC by application of simple reaction-diffusion equations.

DOI: [10.1103/PhysRevB.83.075202](https://doi.org/10.1103/PhysRevB.83.075202)

PACS number(s): 61.72.jj, 61.82.Fk, 66.30.Lw

I. INTRODUCTION

Silicon carbide (SiC) in various forms is considered a promising structural material for nuclear,^{1,2} electronic, and optoelectronic device applications³ because of its high thermal stability, excellent resistance to chemical attack, high thermal conductivity, and high electron saturation drift velocity. While in use or production, SiC is subjected to neutron irradiation or ion irradiation of dopants, which can produce the Frenkel pairs both in the silicon and carbon sublattices in addition to clustered defects and antisite defects.^{4,5} Very few experimental results are available for the interstitial motion in SiC due in part to the experimental difficulty associated with resolving extremely small clusters in this system. However, it is accepted that interstitials play an important role both in the damage accumulation and in the early stages of the thermal recovery processes. Two distinct recovery stages of the electrical resistivity for neutron-irradiated 3C-SiC, the polytype of particular importance in nuclear applications, have been observed at 150 and 300 °C.⁶ An additional recovery stage for the amorphized 6H-SiC, the polytype of special importance in device applications, has been observed at 300–450 °C using channeling Rutherford backscattering spectrometry.⁷ The estimated activation energies of 0.3 ± 0.15 eV for the first stage and 0.74 ± 0.05 eV for the second stage were considered to be related to the recombination process of close Frenkel pairs and the diffusion of carbon interstitials, respectively. The measured activation energy of 1.5 ± 0.3 eV for the third stage was suspected to be the migration energy of silicon interstitials; recent theoretically simulated values of 1.4–1.5 eV support this position.^{8,9} However, the wide variety of potential recovery-process routes makes it difficult to identify the relative contributions of specific defects to the observed annealing. The fundamental studies on the motion of both the interstitial and the vacancy, including the very basic formation and migration energies, have been limited largely to theoretical simulation using methods such as *ab initio*,⁹ molecular dynamics with empirical potentials,⁸ or Monte Carlo simulations,¹⁰ although these methods provide temporally and spatially limited knowledge.

Since transmission electron microscopy (TEM) essentially provides direct evidence of the resultant defect microstructures after defect evolution over a macroscopic time scale, the technique is often employed to investigate the secondary defects

formed during neutron exposure. Understanding the defect motion is crucial to be able to describe the response of SiC to irradiation damage and any thermal recovery process. Although it is difficult to understand the motion of isolated interstitials and vacancies from the defects themselves, the information of the point-defect motion, which is a thermally activated process, can be obtained from the irradiation-temperature-dependent variation of the defect microstructures such as the denuded-zone (DZ) width of irradiation-produced defects near point-defect sinks.^{11,12} In this paper, the temperature-dependent DZ width along the grain boundaries in neutron-irradiated SiC was quantitatively analyzed to determine the activation energy of interstitial migration. In addition, the migration energy of silicon interstitials will be estimated based on the simple kinetic equations at the pseudo-steady state following the methodology used by Zinkle.¹¹

II. EXPERIMENTAL PROCEDURE

The material used for this work was polycrystalline β -SiC, which was produced by chemical vapor deposition by Rohm and Haas Advanced Materials (Woburn, Massachusetts).¹³ The chemical-vapor deposited (CVD) material is extremely pure, with typical total impurity concentration of less than 5 wppm. The grain width is between 5 and 10 μm in the plane parallel to the deposition substrate, with the grains elongated in the $\langle 111 \rangle$ growth direction perpendicular to the substrate. The material is typically free of microcracks or other large flaws, but atomic layer stacking faults on the $\{111\}$ planes are common. There is no porosity in this CVD SiC, and the material essentially has theoretical density (approximately 3.21 g/cm³).

Samples were irradiated in the High Flux Isotope Reactor at Oak Ridge National Laboratory. Six SiC samples irradiated at temperatures of 1010, 1050, 1130, 1220, 1300, and 1380 °C were selected from a series of specimens irradiated at a fixed-core capsule containing 10 subcapsules to investigate the temperature dependence of the denuded-zone width. The fluence for the specimen studied here ranged from 1.4×10^{25} to 1.9×10^{25} n/m² ($E > 0.1$ MeV). Irradiation temperatures were estimated by post-irradiation viewing of melt wires inserted in both ends of each subcapsule. A detailed description of the irradiation experiment can be found in Ref. 14.

Specimens of 5.8 mm diameter with 0.5 or 3.2 mm thickness were axially cut in thin strips and mechanically polished to

TABLE I. Microstructural parameters in neutron-irradiated 3C-SiC, which are measured in the regions well away from grain boundaries. The radius and the number density of TEM invisible voids theoretically detected using the Eqs. (5) and (6) are also listed below 1130 °C.

Irradiation temperature (°C)	Temperature error		DZ width (nm)	Loop radius (nm)	Loop density (m ⁻³)	Void radius (nm)	Void density (m ⁻³)	Void radius estimated by Eqs. (5) and (6) (nm)	Void density estimated by Eqs. (5) and (6) (m ⁻³)
	+	-							
1010	20	20	8.9	1.1	1.9×10^{23}	Not detected	Not detected	0.2	6.8×10^{24}
1050	40	40	12	1.2	1.1×10^{23}	Not detected	Not detected	0.2	4.0×10^{24}
1130	60	60	17	2.2	9.1×10^{22}	0.5	1.8×10^{20}	0.7	4.9×10^{23}
1220	60	60	22	2.2	1.2×10^{23}	0.5	3.8×10^{22}	-	-
1300	30	30	43	3.8	6.5×10^{22}	0.6	5.5×10^{22}	-	-
1380	45	45	57	8.2	7.1×10^{21}	0.7	8.1×10^{22}	-	-

~30 μm thickness. Thin foils were prepared in a commercial Ar-ion-milling unit (FISCHIONE model 1010) using a (3–5)-keV dual-ion beam. Microstructures were studied using a transmission electron microscope (Philips/FEI Technai 20, 200 keV). Thickness determinations of TEM thin foils were made at several locations by measurement of the projected width of the stacking faults. The loop DZ width, which was defined here as a mean distance from a loop edge to the nearest grain boundary, was averaged over 800 nm in total length of three to five random grain boundaries with different misorientations.

III. RESULTS

Both the unirradiated and irradiated CVD SiC contain several types of grain boundaries with different misorientation. Nevertheless, neighboring grains have similar growth orientation associated with the columnar structure characteristic of the CVD materials. No significant grain growth was observed as a result of the irradiation. Typical TEM images of the dislocation loop DZ formed along several types of grain boundaries in SiC irradiated to 1.9×10^{25} n/m² at 1380 °C are shown in Fig. 1. The grain boundary marked GB 1 shown in Fig. 1(a) is a straight tilt boundary, and the rotation angle and axis are determined to be 35.3° and parallel to $[\bar{0}.08, 1, 1.08]$, respectively, by analysis of Kikuchi patterns obtained from both the grains. Other examples of random boundaries containing both the tilt and twist components are shown in Figs. 1(b) and 1(c). The suggested misorientations were 28.9°/ $[\bar{1}.0, 0.71, 0.79]$ for GB 2 in Fig. 1(b) and 30.2°/ $[\bar{0}.64, 1, 0.32]$ for GB 3 in Fig. 1(c). An example of coherent boundaries is shown in Fig. 1(d), where the twin boundary with the misorientation of 70.5°/ $[011]$ is imaged using the beam direction close to $[011]$. The inset image of the combined diffraction pattern obtained from both the grains shows typical twin spots along with $[\bar{1}\bar{1}1]$ direction. Although differences of up to ~10% in the mean DZ width were measured within five random grain boundaries irradiated at 1380 °C, this is not considered significant to the grain-boundary type and/or misorientation angles. By contrast, no, or very limited, DZ were observed along the coherent boundaries such as twin boundaries as is evident from Fig. 1(d).

The loop DZ observed along grain boundaries in SiC irradiated with neutrons at six different irradiation temperatures is shown in Fig. 2. This series shows a positive temperature dependence of the DZ width, where the smallest DZ width of 8.9 nm was observed in SiC irradiated at 1010 °C and the largest of 57 nm was observed at 1380 °C. Results of the quantitative analysis on the DZ width and defect microstructures examined in the regions well away from the DZ are summarized in Table I. Most loops were identified as Frank faulted loops formed on $\{111\}$ crystallographic planes by means of *gb* contrast analysis and imaging from 111 rel-rods (reciprocal lattice rod). Loops formed in some grains are not imaged because of the off-Bragg condition. The loop density decreased and the size gradually increased with increasing temperature below 1300 °C; both the rapid decrease in number density and rapid increase in size were observed above this temperature. The preferential formation of small voids at or near the twin boundaries were observed above 1130 °C. Voids formed in matrix regions become visible above 1220 °C. Although the mean void size is less dependent on the irradiation temperature, the number density of visible voids strongly depends on the temperature.

The local loop number densities are plotted against the distance from grain boundaries at each temperature in Fig. 3, where the horizontal dotted lines show the bulk loop density. The loop number density rapidly reaches the bulk density in the very small regions near the end of loop DZ below 1220 °C. Above 1300 °C, the loop number density increased moderately even beyond the DZ until the bulk density was achieved. The loop size was nearly independent of the distance from the grain boundary at all the irradiation temperatures.

IV. DISCUSSION

The formation of dislocation loop DZ along grain boundaries, where the concentration of a point defect is always lower than the critical concentration for forming defect aggregates, has been reported for many irradiated materials.^{11,15,16} In the absence of any impurity effects, the sink efficiency of the grain boundary may depend on the degree of lattice disorder resulting from the grain mismatch. Indeed, variation of the DZ width dependent on the misorientation angle was reported

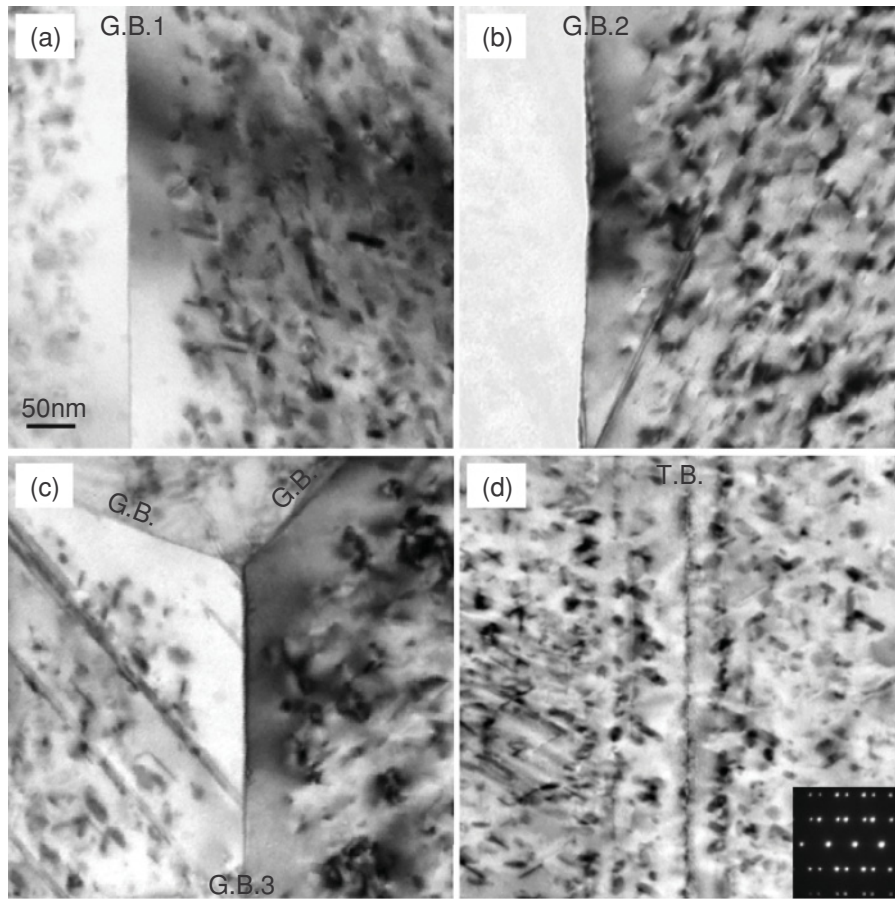


FIG. 1. Loop denuded zone observed along several types of grain boundaries in SiC irradiated at 1380 °C: (a) straight tilt boundary with the misorientation of $35.3^\circ/[0.08, 1, \bar{1}.08]$, (b) random grain boundary with the misorientation of $28.9^\circ/[1, 0.71, 0.79]$, (c) grain-boundary triple junction, and (d) twin boundary with the misorientation of $70.5^\circ/[011]$ and the twin diffraction spots for the inset image.

for both the interstitial- and vacancy-type defect clusters.¹⁷ For some materials, however, the DZ width was reported to be insensitive to the misorientation angles of random grain boundaries.¹⁸ In any case, most observations showed no, or very limited, denudation at the coherent boundaries and those are believed to be poor point-defect sinks. In our study, no notable relationship between DZ width and misorientation angles was observed except for coherent twin boundaries, indicating nearly equal sink efficiency of the random grain boundaries in CVD SiC. Therefore, all of the random grain boundaries were treated as the point-defect sink having the same sink efficiency, hereafter, and coherent boundaries were excluded from further discussion.

Very dense black spots and/or small loops, which are aggregates of point defects, are the dominating defect microstructures in SiC irradiated with neutron or self-ion in the wide temperature range.^{2,19,20} In this study, quantitative results of their size and bulk number density showed a good agreement with the previous reports. The loops were identified or speculated to be of interstitial type in Ref. 21. The absence of vacancy-type loops implies the existence of tiny three-dimensional clusters of vacancies for the temperatures studied here, although the number density of “TEM visible” voids was zero at 1010 °C or very limited at 1050 °C. This is supported by the reports showing void formation in SiC at 4.9 dpa, 1050 °C in a neutron study²⁰ and 10 dpa, 1000 °C in a self-ion study.¹⁹ Note that the population of loops and voids was reported to be nearly saturated by 1 dpa at the irradiation temperature below

1460 °C.²⁰ In a condition in which most vacancies are no longer isolated, recombination terms can be ignored and the sink strength, which depends strongly on the population of vacancy clusters, may be assumed constant. Then, the steady-state reaction-diffusion equation near the one-dimensional sinks such as grain boundary is conventionally given as

$$D_i \frac{d^2 C_i}{dx^2} - D_i C_i k_{\text{Total}}^2 + G = 0, \quad (1)$$

where D_i (m^2s^{-1}) is the interstitial diffusion coefficient, C_i is the interstitial concentration, k_{Total}^2 (m^{-2}) is the temperature-dependent total sink strength, G (s^{-1}) is the generation rate of point defects, and x (m) is the distance from a grain-boundary surface. The grain boundaries are assumed to be continuously unsaturated with the migrating point defects (in other words, treated as a perfect sink) in accordance with a generally accepted boundary condition. Since the thermal concentration of the interstitials at the grain boundary is extremely limited compared to the bulk concentration during irradiation, C_i can be set to zero at the grain-boundary surface. Based on the assumptions above, the critical concentration required so that the average loop growth rate is positive may be solved at $x = L$ as follows:

$$C_i^{\text{crit}} = C_i^\infty [1 - \exp(-L\sqrt{k_{\text{Total}}^2})], \quad (2)$$

where C_i^∞ is the bulk concentration of interstitials and L (m) is the DZ width. The interstitial concentration far from the grain boundary C_i^∞ should be constant at $\frac{G}{D_i k_{\text{Total}}^2}$ under the

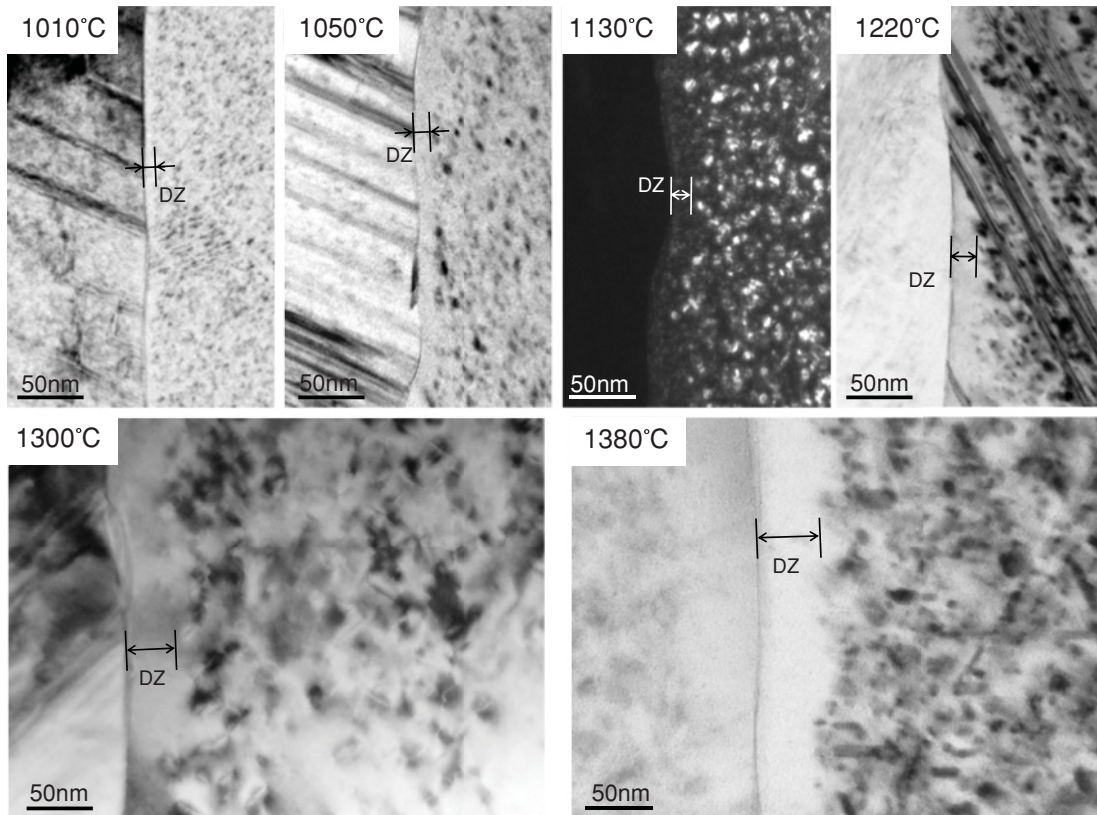


FIG. 2. Irradiation temperature dependence of the width of the loop denuded zone formed along random grain boundaries.

pseudo-steady state. Then, the equation (2) may be rewritten as

$$D_i = \frac{G[1 - \exp(-L\sqrt{k_{\text{Total}}^2})]}{C_i^{\text{crit}}k_{\text{Total}}^2}. \quad (3)$$

It is clear that the sink strength is essential for obtaining the interstitial diffusion coefficient. When all the defects have enough size to detect by TEM as in the case above 1220 °C, the total sink strength can be estimated from the equations

$$k_L^2 = 2\pi r_L N_L, \quad k_V^2 = 4\pi r_V N_V, \quad (4)$$

where r (m) is the mean radius and N (m^{-3}) is the number density of loops or voids. If this is not the case, additional simplifications of the relationship between sink strength and DZ width may be required as discussed below.

In a case such that the loop number density rapidly reaches the matrix level at a short distance from the grain boundary, the interstitial concentration reach to the C_i^{crit} just before the distance where C_i^∞ is practically achieved. The total sink strength may then be given by

$$k_{\text{Total}}^2 \approx \frac{1}{L^2}. \quad (5)$$

In the experimental conditions studied here, Eq. (5) is likely applicable at the temperatures below 1130 °C because of the small DZ width and the rapid increase in the loop density near the location at $x = L$ (see Fig. 3). Indeed, the n_v ($n_v = N_V 4\pi r_V^3 b / 3\Omega$) experimentally estimated from voids observed by TEM is much lower than the experimentally

estimated n_i ($n_i = N_L \pi r_L^2 b / \Omega$) at <1130 °C, indicating the number density of voids would be underestimated. In an attempt to prove the reliability of the simplifications, the size and population of missing defects of TEM invisible voids were estimated from the sink strengths obtained using Eq. (5) in the following way. Assuming the number of vacancies constituting voids is same as the number of interstitials constituting loops observed by TEM, Eq. (4) can be rewritten as

$$k_L^2 = \frac{2n\Omega}{r_L b}, \quad k_V^2 = \frac{3n\Omega}{r_V^2}, \quad (6)$$

respectively, where n is the number of interstitials or vacancies constituting clusters ($n = n_i = n_v$), Ω (m^3) is the atomic volume, and b (m) is Burgers vector. The parameters of TEM invisible voids estimated from Eqs. (5) and (6) are listed in Table I for the temperatures below 1130 °C. The void radii were estimated to be 0.2 nm at <1050 °C and 0.7 nm at 1130 °C; these are reliable values considering the temperature dependency and TEM resolution limit with satisfactory accuracy in this paper. It supports the fact that the simplifications and assumptions employed here are reasonable to our experimental conditions. The estimated number densities of the TEM invisible voids are much higher than the loop densities at these temperatures. Therefore, one can conclude that the vacancies start to migrate below 1010 °C, and the stabilized, very small voids dominate both the sink strength and the loop DZ width at least up to 1130 °C.

Calculated diffusion coefficients of interstitials from Eq. (3) are plotted against reciprocal temperatures in Fig. 4.

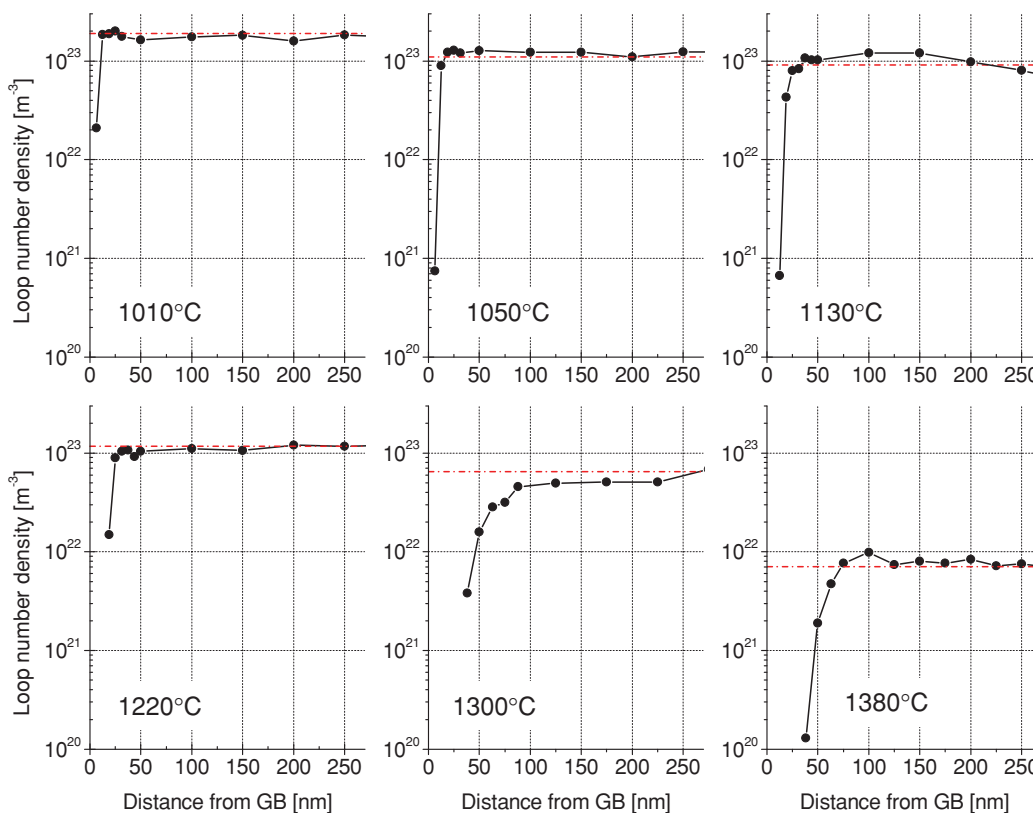


FIG. 3. (Color online) Distance-dependent loop number density.

The C_i^{crit} was assumed as 10^{-14} as has been conventionally utilized by Zinkle.¹¹ The generation rates of point defects, which ranged from $1.5\text{--}2.7 \times 10^{-7} \text{ s}^{-1}$ depending on the total fluence, were estimated using the conventional cascade efficiency of 30% = n/n^* (n^* = number of originally displaced atoms). The error bars for plotted diffusivities were estimated based on the sum of uncertainty of the defect number density, because the errors for other parameters such as defect size and DZ width were negligibly small compared with the accuracy of foil-thickness determinations. These error bars do not provide any assurance that the absolute values of the diffusion coefficient are within the error range because of the use of the conventional C_i^{crit} value and cascade efficiency. However, the slope of the fitted line, which is corresponding to the activation energy of the interstitial motion, is independent of these temperature-independent values. Note that the actual error for the relative temperature would be expected to be minimal, although the somewhat large temperature errors for each plot are shown in Fig. 4. In the absence of significant errors for the relative irradiation temperatures, the slope of the fitted line is less sensitive to the deviation of the irradiation temperatures within the absolute errors. The loops formed in SiC, which is somewhat of an ionic compound, should maintain their stoichiometric structure.^{21,22} The influx of Si interstitials has been pointed out as a parameter responsible for controlling the loop growth rates due to both the smaller displacement rates and mobility compared with C interstitials.²³ On the basis of this, the obtained activation energy of 1.5 eV possibly corresponds to the migration energy of slower-moving Si interstitials. The potential error was estimated at ± 0.1 eV

for the activation energy on the basis of the potential errors discussed above. In the theoretical simulation by Gao *et al.*, the migration energy of 1.53 ± 0.02 eV has been reported for Si interstitials in 3C-SiC,⁸ which is comparable to our

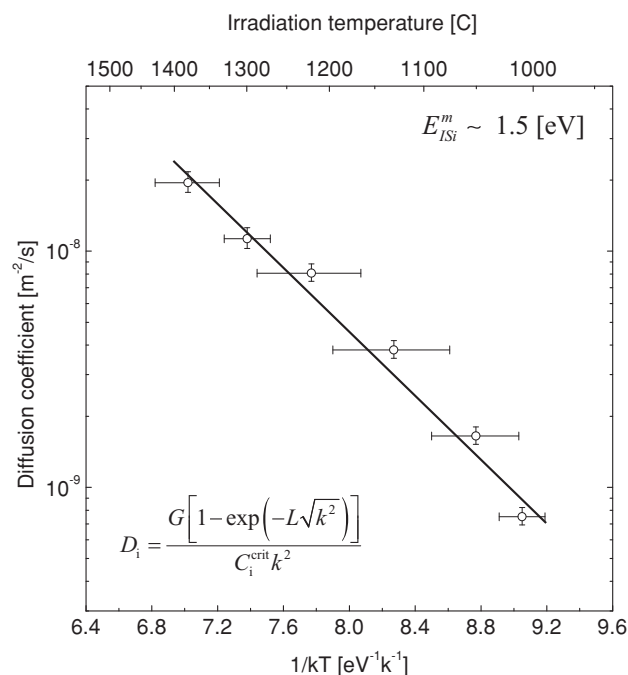


FIG. 4. Arrhenius plots of the diffusion coefficient estimated by Eq. (3).

result. Therefore, our result also supports that the activation energies for the third recovery stage in the disordered Si sublattice observed by Weber⁷ may be attributed to the long-range migration of the Si interstitial, although some other recovery stages at lower temperatures, likely associated with the close Frenkel pairs, C interstitials, and some other migration pathways with energy barriers lower than 1 eV,²⁴ were observed.

V. CONCLUSION

In order to obtain the information about the interstitial motion in SiC, the temperature-dependent width of the interstitial loop denuded zone (DZ) formed along the random grain boundaries was evaluated. No relationship between DZ width and grain-boundary misorientations were detected except for coherent twin boundaries showing no, or very limited, DZ width. The quantitative analysis showed a positive temperature dependence of the DZ width, where the smallest DZ width of 8.9 nm was observed in SiC irradiated at 1010 °C and

the largest of 57 nm was observed at 1380 °C. Significant populations of small TEM invisible voids ($r_v = 0.2\text{--}0.7$ nm) were theoretically found to be formed in specimens irradiated below 1130 °C based on a simple reaction-diffusion equation, which were supposed to be limiting the interstitial motion at lower temperatures. The temperature-dependent diffusion coefficient estimated from the loop-denuded width showed an activation energy of interstitial migration of 1.5 ± 0.1 eV in SiC, which is likely associated with the slower-moving species of Si interstitials. The very limited experimental results of the activation energy for the thermal recovery process and the simulation results well support this.

ACKNOWLEDGMENTS

This research was supported by the Office of Fusion Energy Sciences, U.S. Department of Energy under Contract No. DE-AC05-00OR22725 with UT-Battelle, LLC. Materials used in this work were irradiated in the High Flux Isotope Reactor, a DOE user facility.

*Corresponding author: Currently at Institute of Advanced Energy, Kyoto University Gokasho, Uji, Kyoto 611-0011, Japan, kondo@iae.kyoto-u.ac.jp.

¹Y. Katoh, L. L. Snead, C. H. Henager Jr., A. Hasegawa, A. Kohyama, B. Riccardi, and H. Hegeman, *J. Nucl. Mater.* **367**, 659 (2007).

²L. L. Snead, T. Nozawa, Y. Katoh, T. S. Byun, S. Kondo, and D. A. Petti, *J. Nucl. Mater.* **371**, 329 (2007).

³Z. C. Feng, A. J. Mascarenhas, W. J. Choyke, and J. A. Powell, *J. Appl. Phys.* **64**, 3176 (1988).

⁴J. M. Perlado, L. Malerba, A. Sanchez-Rubio, and T. Diaz de la Rubia, *J. Nucl. Mater.* **276**, 235 (2000).

⁵F. Gao and W. J. Weber, *Phys. Rev. B* **66**, 024106 (2002).

⁶V. Nagesh, J. W. Farmer, R. F. Davis, and H. S. Kong, *Appl. Phys. Lett.* **50**, 1138 (1987).

⁷W. J. Weber, W. Jiang, and S. Thevuthasan, *Nucl. Instrum. Methods Phys. Res. B* **166-167**, 410 (2000).

⁸F. Gao, W. J. Weber, M. Posselt, and V. Belko, *Phys. Rev. B* **69**, 245205 (2004).

⁹M. Bockstedte, A. Mattausch, and O. Pankratov, *Phys. Rev. B* **68**, 205201 (2003).

¹⁰Z. Rong, F. Gao, W. J. Weber, and V. Belko, *J. Appl. Phys.* **102**, 103508 (2007).

¹¹S. J. Zinkle, in *Effects of Radiation on Materials: 15th International Symposium*, edited by R. E. Stoller, A. S. Kumar, and D. S. Gelles

(American Society for Testing and Materials, Philadelphia, 1992).

¹²M. Kiritani, *J. Nucl. Mater.* **216**, 220 (1994).

¹³[<http://www.cvdmaterials.com>].

¹⁴L. L. Snead, Y. Katoh, and S. Connery, *J. Nucl. Mater.* **367**, 677 (2007).

¹⁵B. N. Singh and A. J. E. Foreman, *Philos. Mag.* **29**, 847 (1974).

¹⁶M. F. Ashby, *Scr. Metall.* **3**, 837 (1969).

¹⁷R. W. Siegel, S. M. Chang, and R. W. Balluffi, *Acta Metall.* **28**, 249 (1980).

¹⁸B. K. Basu and C. Elbaum, *Acta Metall.* **13**, 1117 (1965).

¹⁹Y. Katoh, N. Hashimoto, S. Kondo, L. L. Snead, and A. Kohyama, *J. Nucl. Mater.* **351**, 228 (2006).

²⁰S. Kondo, Y. Katoh, and L. L. Snead, *J. Nucl. Mater.* **382**, 160 (2008).

²¹L. W. Hobbs, A. E. Hughes, and D. Pooley, *Proc. R. Soc. London, Ser. A* **332**, 167 (1973).

²²L. W. Hobbs, F. W. Clinard Jr., S. J. Zinkle, and R. C. Ewing, *J. Nucl. Mater.* **216**, 291 (1994).

²³S. Kondo, Y. Katoh, and A. Kohyama, in *Mechanical Properties and Performance of Engineering Ceramics and Composites III*, edited by E. Lara-Curzio (The American Ceramic Society, Ohio, 2007).

²⁴M. Bockstedte, A. Mattausch, and O. Pankratov, *Phys. Rev. B* **68**, 205201 (2003).